



Universiteit
Leiden

The Netherlands

Multimodality Imaging of Anatomy and Function in Coronary Artery Disease

Schuijf, J.D.

Citation

Schuijf, J. D. (2007, October 18). *Multimodality Imaging of Anatomy and Function in Coronary Artery Disease*. Retrieved from <https://hdl.handle.net/1887/12423>

Version: Corrected Publisher's Version

License: [Licence agreement concerning inclusion of doctoral thesis in the Institutional Repository of the University of Leiden](#)

Downloaded from: <https://hdl.handle.net/1887/12423>

Note: To cite this publication please use the final published version (if applicable).

Chapter 5

Meta-Analysis of Comparative Diagnostic Performance of Magnetic Resonance Imaging and Multi-Slice Computed Tomography for Non-Invasive Coronary Angiography

Joanne D. Schuijf, Jeroen J. Bax, Leslee J. Shaw, Albert de Roos, Hildo J. Lamb, Ernst E. van der Wall, William Wijns

Abstract

Background

Magnetic Resonance Imaging (MRI) and Multi-Slice Computed Tomography (MSCT) have emerged as potential non-invasive coronary imaging techniques. The objective of the present study was to clarify the current accuracy of both modalities in the detection of significant coronary artery lesions (compared to conventional angiography as the gold standard) by means of a comprehensive meta-analysis of the presently available literature.

Methods

A total of 51 studies on the detection of significant coronary artery stenoses (50% diameter stenosis or more) and comparing results to conventional angiography were identified by means of a MEDLINE search. Weighted sensitivities, specificities, predictive values, all with 95% confidence intervals (CIs), as well as summary odds ratios were calculated for both techniques. In addition, the relationship between diagnostic specificity and disease prevalence was determined using meta-regression analysis.

Results

A comparison of sensitivities and specificities revealed significantly higher values for MSCT (weighted average: 85%, 95% CI: 86%-88% and 95%, 95% CI: 95%) as compared with MRI (weighted average: 72%, 95% CI: 69%-75% and 87%, 95% CI: 86-88%). A significantly higher odds ratio (16.9-fold) for the presence of significant stenosis was observed for MSCT as compared to MRI (6.4-fold) ($p < 0.0001$). Linear-regression analysis revealed a better specificity for MSCT versus MRI in lower disease prevalence populations ($p = 0.056$).

Conclusion

Meta-analysis of the available studies with MRI and MSCT for non-invasive coronary angiography indicates that MSCT has currently a significantly higher accuracy to detect or exclude significant CAD.

Introduction

In the western world, coronary artery disease (CAD) remains the leading cause of death and its prevalence is still increasing. The current gold standard for the detection of CAD, invasive coronary angiography (CAG), allows direct visualization of the coronary lumen with high spatial and temporal resolution. However, it is an invasive procedure with several important drawbacks, including the significant costs and a small risk of serious complications^{1,2}. Furthermore, in a substantial number of procedures, no evidence of clinically important CAD is demonstrated. In patients with a low to intermediate pre-test likelihood of CAD, therefore, non-invasive evaluation of the coronary arteries would be highly desirable, whereas direct referral for invasive CAG may still be preferred in patients with a high pre-test likelihood.

Over the past decade, Magnetic Resonance Imaging (MRI) and, more recently, Multi-Slice Computed Tomography (MSCT) have emerged as non-invasive cardiac imaging techniques. Their rapid development has led to the expectation that both techniques can be applied in the detection of CAD by direct visualization of coronary artery stenoses (instead of the detection of their functional consequences). However, which technique is more likely to be implemented in the diagnostic workup of patients with suspected CAD eventually, still remains a heated issue of debate.

To evaluate the accuracies of MRI and MSCT in the detection of CAD, we performed a comprehensive meta-analysis of the presently available literature on MRI and MSCT in the detection of significant coronary artery stenoses.

Methods

Review of published reports

The objective of the current analysis was to evaluate the available reports on the diagnostic accuracy of MSCT and MRI in the detection of CAD. The studies were identified by means of several search strategies:

1. A search of the MEDLINE database (January 1990 –January 2005) was performed using the following keywords: computed tomography, magnetic resonance imaging, coronary artery disease, stenosis, occlusion, detection, and angiography.
2. A manual search of cardiology and radiology journals (*American Heart Journal, American Journal of Cardiology, Circulation, European Heart Journal, European Journal of Radiology, Heart, Journal of the American College of Cardiology, Journal of Magnetic Resonance Imaging, Magnetic Resonance Imaging, Magnetic Resonance in Medicine, Radiology*) from 1990 to 2005.
3. Reference lists from the cited manuscripts were screened for additional studies that may have been missed.

Only articles performing a head-to-head comparison between non-invasive angiography with either MRI or MSCT and invasive CAG in patients with known or suspected CAD were considered for

Table 1. Diagnostic accuracy of MRI to detect coronary artery stenoses in 28 studies with 903 patients.

Year	Author	Pts (n)	Mean age (yrs)	Male (%)	Prevalence of CAD (%)	CAG criterion	Technique	Assessable (%) (nr segments)	Sensitivity (%) (nr segments)	Specificity (%) (nr segments)
2D Breath Hold										
1993	Manning et al. ²⁴	39	54	90	74	> 50 V*	GE	98 (147/150)	90 (47/52)	92 (87/95)
1993	Pennell et al. ²⁶	7	NA	NA	71	# V*	GE	NA	83 (5/6)	NA
1996	Mohiaddin et al. ²⁵	16	57	NA	NA	> 50 V*	GE	90 (43/48)	56 (5/9)	82 (28/34)
1996	Pennell et al. ²⁵	39	55	92	NA	> 50 V	GE	NA	85 (47/55)	NA
1997	Postel et al. ²⁸	35	58	77	NA	> 50 V*	GE	89 (123/140)	63 (12/35)	89 (80/90)
Weighted mean										
								93 (315/338)	80 (126/157)	89 (195/219)
3D Breath Hold										
1999	Kessler et al. ¹⁰¹	6	NA	NA	NA	> 50 V	GE	NA	60 (3/5)	NA
2000	Van Geuns et al. ³⁰	38	NA	71	68	> 50 V	GE	69 (187/272)	68 (21/31)	97 (151/156)
2000	Regentus et al. ³²	50	61	80	72	> 50 V	GE	77 (268/350)	86 (48/56)	91 (193/212)
2002	Regentus et al. ³¹	32	58	72	69	> 50 V	GE	76 (171/224)	87 (28/30)	91 (129/141)
2004	Jahnke et al. ⁷¹	40	62	60	63	> 50 V	SSFP	45 (143/320)	63 (12/19)	82 (102/124)
Weighted mean										
								66 (769/1166)	78 (110/141)	91 (575/633)
3D Navigator										
1996	Post et al. ¹⁴	20	58	80	75	> 50 V	GE	96 (77/80)	38 (8/21)	95 (53/56)
1997	Muller et al. ¹²	35	61	71	86	> 50 V	SE	NA	83 (45/54)	94 (115/122)
1997	Kessler et al. ⁹	73	60	75	NA	> 50 V	GE	52 (236/455)	65 (28/43)	88 (169/193)
1998	Woodard et al. ²²	10	60	50	NA	> 30 V*	GE	NA	70 (7/10)	NA
1999	Sandstede et al. ¹⁶	30	63	72	100	> 50 V*	SE	77 (92/120)	81 (30/37)	89 (49/55)
1999	Van Geuns et al. ¹⁸	32	NA	62	NA	> 50 V	GE	74 (151/203)	50 (13/26)	91 (114/125)
1999	Kessler et al. ¹⁰¹	6	NA	NA	NA	> 50 V	GE	NA	60 (3/5)	NA
2000	Sardanelli et al. ¹⁷	42	65	79	87	> 50 V	GE	86 (234/273)	82 (55/67)	89 (149/167)
2001	Kim et al. ¹¹	109	59	69	59	> 50 OV*	GE	86 (374/434)	83 (78/94)	73 (204/280)
2002	Plein et al. ¹³	11	61	80	100	> 50 V	GE	93 (37/40)	88 (15/17)	85 (17/20)
2002	Weber et al. ²⁰	11	61	80	NA	> 50 V	SE	70 (62/88)	88 (14/16)	93 (43/46)
2002	Whittinger et al. ²¹	25	62	80	NA	# V	TFE	85 (102/120)	75 (18/24)	100 (78/78)
2002	Regentus et al. ¹⁵¹	32	58	72	69	> 50 V	TFE	69 (155/224)	60 (15/25)	88 (115/130)
2002	Metanabe et al. ¹⁹	12	71	75	100	> 50 V	TFE	70 (49/70)	80 (12/15)	85 (29/34)
2002	Van Geuns et al. ²³	27	59	70	70	> 50 V	TFE	69 (139/201)	46 (12/26)	90 (102/113)
2003	Bogaert et al. ²	21	62	71	68	> 50 Q	TFE	72 (134/186)	56 (15/27)	83 (69/107)
2003	Konken et al. ³	69	58	63	68	> 50 Q*	GE	84 (233/276)	73 (68/85)	62 (62/148)
2004	Jahnke et al. ⁷¹	40	62	60	63	> 50 V	SSFP	79 (254/320)	72 (28/56)	92 (230/248)
2005	Gerbner et al. ⁶	27	65	89	81	> 50 Q	TFFE	100 (294/294)	62 (38/58)	84 (198/236)
2004	Muller et al. ³	30	60	83	100	> 50 NA	GE	100 (221/221)	85 (52/61)	84 (151/180)
2005	Sommer et al. ⁴	18	63	61	61	> 50 Q	TFE	87 (109/126)	87 (34/41)	88 (80/91)
Weighted mean										
								82 (2953/3731)	73 (543/744)	85 (2047/2399)
3T										
2005	Sommer et al. ⁴	18	63	61	61	> 50 Q	TFE	86 (108/126)	82 (14/17)	89 (80/90)
Weighted mean 1.5T										
								83 (3441/4147)	72 (749/1043)	87 (2600/2997)

* Only vessels available, no segmental analysis; † Same study group. In case of study comparing 2 techniques, results of technique with best results were included in the overall weighted mean. Abbreviations: CAG: conventional angiography; GE: gradient echo; NA: not available; Q: quantitative analysis; SE: spin-echo; SSFP: steady-state free precession; TFE: turbo flash echo; TFFE: turbo flash field echo; V: visual analysis

evaluation, while abstracts, reviews and articles written in another language than English were disregarded. Finally, reports indicating that the patients included were subsets of previously published studies (n=1) or reports with insufficient data to calculate sensitivity and specificity on a segmental basis (n=9) were also excluded. When papers reported results of multiple observers, data from the observer with the highest accuracy were used for further analysis.

Statistical Methods

From each publication, a 2 x 2 frequency table was constructed based upon true negative and positives and false negative and positives. Diagnostic sensitivity (= true positives / [true positive + false negatives]) and specificity (= true negatives / [true negatives + false positives]) were calculated. Pooled calculations for diagnostic accuracy of MRI and MSCT techniques were performed based upon the proportional sample size of each report. The 95% confidence intervals (CIs) of the weighted sensitivities and specificities were calculated using the following formula: $p \pm 1.96 \cdot \sqrt{\{p \cdot (100-p)\} / n}$, where p = weighted sensitivity or specificity (%) and n = the total number of segments.

Summary odds ratios were calculated using the Comprehensive Meta Analysis™ program (www.meta-analysis.com, access date: February 2004). The odds ratio and summary odds ratio, with 95% CIs, for angiographic CAD was defined for positive MSCT and MRI studies. For this analysis, only data with negative and positive study findings were included. Pooled summary data for CAD incident cases/denominators of negative and positive studies were also calculated. A chi-square test for heterogeneity was calculated. The summary odds ratio was calculated using a random effects inverse variance approach. Analysis of variance techniques were also applied to compare the effect size for MSCT versus MRI.

To compare the relationship between accuracy and disease prevalence, a meta-regression analysis was performed. For MSCT, a univariable meta-regression was performed estimating the influence of diagnostic specificity on CAD prevalence. Use of multivariable regression analyses did not alter the univariable relationship but were performed and included the prevalence of males and average age of the population. From this model, a linear regression model was employed to calculate the correlation and beta coefficients.

Diagnostic sensitivity and specificity was compared for intermediate and high-risk groups by employing analysis of variance techniques. Using a general linear model, the average diagnostic sensitivity and specificity for intermediate and high-risk groups was compared for MSCT and MRI; weighted by average sample size. A p-value <0.05 was considered statistically significant.

Table 2. Diagnostic accuracy of MSCT to detect coronary artery stenoses in 24 studies with 1300 patients.

Year	Author	Pts (n)	Mean age (yrs)	Male (%)	Prevalence of CAD (%)	CAG criterion	BB-use	Assessable (%) (nr segments)	Sensitivity (%) (nr segments)	Specificity (%) (nr segments)	
4-slice											
2001	Achenbach et al. ³¹	64	63	75	NA	> 50, Q*	NA	68 (174)	85 (40/47)	76 (96/127)	
2001	Knez et al. ³²	44	NA	86	70	> 50, V	No	93 (358)	78 (39/50)	98 (30/1308)	
2002	Nieman et al. ³⁸	53	56	75	62	> 50, Q	No	70 (358)	82 (42/51)	93 (28/307)	
2002	Becker et al. ³²	28	64	96	64	> 50, V	No†	95 (187)	81 (21/26)	90 (145/161)	
2002	Vogl et al. ⁴⁶	64	56	56	NA	> 50, V	No	100 (1039)	75 (59/79)	99 (95/960)	
2002	Nieman et al. ³⁷	78	57	73	75	> 50, Q	Yes	68 (505)	84 (48/57)	95 (424/448)	
2003	Nieman et al. ³⁹	24	64	83	100	> 50, Q	NA	69 (17/29)	90 (71/79)	75 (50/67)	
2003	Morgan-Hughes et al. ³⁶	30	56	80	NA	> 70, Q	No†	68 (140)	72 (18/25)	86 (99/115)	
2003	Leber et al. ³³	91	62	79	67	> 50, V	Yes	80 (653)	81 (72/88)	95 (539/565)	
2004	Kuettner et al. ³⁴	66	61	74	100	> 70, Q	No	57 (487/858)	66 (39/59)	98 (420/428)	
2004	Gerber et al. ⁶	27	65	89	81	> 50, Q	Yes	100 (294/294)	79 (46/58)	71 (168/236)	
8-slice											
Weighted mean											
2004	Martynama et al. ⁴¹	25	63	68	64	> 50, Q	No	74 (258/348)	90 (27/30)	99 (226/228)	
2004	Matsuo et al. ⁴²	25	65	76	76	> 50, Q	Yes	94 (94/100)†	75 (45/60)	96 (177/185)	
Weighted mean											
16-slice											
2003	Ropers et al. ³³	77	58	65	53	> 50, Q*	Yes	88 (270/308)	91 (51/56)	93 (200/214)	
2002	Nieman et al. ⁴³	59	58	90	86	> 50, Q*	Yes	100 (231/231)	95 (82/86)	86 (125/145)	
2004	Kuettner et al. ⁴²	60†	58	73	60	> 50, Q	Yes	100 (728/728)	70 (39/56)	97 (655/672)	
True 16-slice											
2004	Dewey et al. ⁴⁴	34	64	79	NA	> 50, Q*	No	98 (133/136)	88 (37/42)	94 (86/94)	
2004	Moller et al. ⁴⁷	128	59	88	83	> 50, Q	Yes	100 (1384/1384)	92 (216/234)	95 (1092/1150)	
2004	Martuscelli et al. ⁴⁹	64	58	82	67	> 50, Q	Yes	84 (613/729)	89 (83/93)	98 (511/520)	
2004	Hoffmann et al. ⁵⁰	33	57	82	57	> 50, Q	Yes	83 (438/530)	70 (30/43)	94 (371/393)	
2005	Kuettner et al. ⁴⁶	72	64	58	50	> 50, Q	Yes	100 (936/936)	82 (96/117)	98 (805/819)	
2005	Moller et al. ⁵²	51	59	73	63	> 50, Q	Yes	100 (610/610)	95 (61/64)	98 (537/546)	
2005	Schuffel et al. ⁴⁸	45	63	93	98	> 50, V	Yes	94 (298/317)	98 (59/60)	97 (231/238)	
2005	Morgan-Hughes et al. ³¹	58	61	81	56	> 50, V	No	100 (675/675)	83 (75/90)	97 (566/585)	
Weighted mean											
Weighted mean overall											
				87 (11545/13275)				88 (829/941)		96 (5179/5376)	
				85 (13964/1650)				85 (1396/1650)		95 (9064/9511)	

BB-use: additional administration of BB medication prior to data acquisition to reduce heart rates.

* Only vessels available, no segmental analysis.

† Exclusion of patients with heart rates higher than 75 bpm

‡ Of these 60 patients, 4 had previous bypass grafting, sensitivity and specificity data are without these 4 patients.

Abbreviations: BB, beta-blocking medication; CAG, conventional angiography; NA, not available; Q, quantitative analysis; V, visual analysis.

Results

Accuracy of MRI

A total of 28 studies comparing MRI to invasive CAG were analyzed and are summarized in Table 1. In 21 studies, the 3D navigator technique was used³⁻²³, whereas data were acquired during breath-holds in 10 studies^{10,15,24-30}. Analysis of the original data resulted in weighted means for sensitivity and specificity of respectively 72% (95% CI: 69% to 75%) and 87% (86% to 88%) for 1.5 T MRI. Average percentage assessable coronary segments was 83% with a 95% CI of 82% to 84%.

Accuracy of MSCT

The results of the studies that compared either 4-slice MSCT^{6,31-40}, 8-slice^{41,42} or 16-slice MSCT⁴³⁻⁵³ to invasive CAG are summarized in Table 2. For all MSCT studies combined, weighted sensitivities and specificities were 85% (95% CI: 83-87 and 95% (95% CI: 95%). Average percentage segments with diagnostic image quality was 87% (95% CI: 86% to 88%), while a significant increase could be observed from 78% with 4-slice systems to 96% with the more recent 16-slice systems.

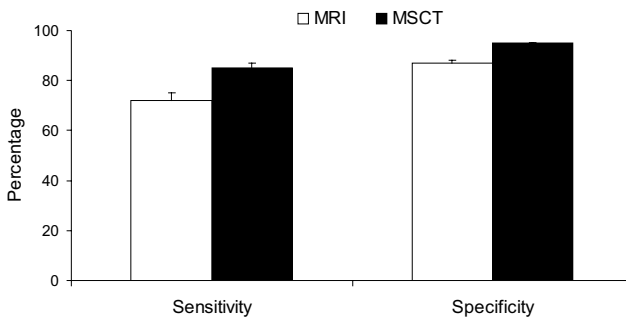


Figure 1. Comparison of sensitivities and specificities of MRI and MSCT in the detection of significant CAD.

Comparison between the 2 techniques

The results of the pooled analysis with the corresponding 95% CIs are summarized in Table 3. In the detection of significant CAD, weighted means for sensitivity, specificity, positive and negative predictive values were higher for MSCT as compared to MRI, without overlap of 95% CIs. Also, the percentage evaluable segments was significantly higher with MSCT as compared to MRI. In Figure 1, sensitivities and specificities of both MRI and MSCT in the detection of coronary artery stenosis are shown.

In a subset analysis of MSCT and MRI, the summary odds ratios and the 95% CIs for the different techniques are plotted in Figure 2. Based upon a combined analysis, the summary odds ratio was elevated 16.9-fold (95% CI: 11.0-26.1) for an abnormal MSCT ($p < 0.0001$), indicating that an abnormal

Table 3. Diagnostic accuracy for the different imaging techniques.

Technique	Sens (%)	95% CI (%)	Spec (%)	95% CI (%)	PPV (%)	95% CI (%)	NPV (%)	95% CI (%)
MRI 2D BH (n = 5)	80	74-86	89	85-93	84	78-90	86	82-91
MRI 3D BH (n = 5)	78	71-85	91	89-93	65	58-72	95	93-97
MRI 3D Navigator (n = 21)	73	70-76	85	84-86	61	58-64	91	90-92
MRI Overall (n = 28)	72	69-75	87	86-88	65	62-68	90	89-91
MSCT 4-slice (n = 11)	80	77-83	94	93-95	67	64-70	97	96-98
MSCT 8-slice (n = 2)	80	72-88	98	97-99	88	81-95	96	94-98
MSCT 16-slice (n = 11)	88	86-90	96	95-97	81	79-83	98	98
MSCT Overall (n = 24)	85	83-87	95	95	76	74-78	97	97
Diagnostic accuracy including uninterpretable segments								
MRI 3D Navigator (n = 8)	59	54-63	71	68-74	40	36-44	84	82-86
MRI Overall (n = 9)	58	53-63	70	68-72	37	33-41	85	83-87
MSCT 4-slice (n = 8)	66	62-70	76	75-77	32	29-35	93	92-94
MSCT 16-slice (n = 10)	85	83-87	94	93-95	71	68-74	97	97
MSCT Overall (n = 18)	77	75-79	94	93-95	51	49-53	96	96

BH: breath hold; CI: confidence interval; PPV: positive predictive value; NPV: negative predictive value
Number in parentheses represents number of studies.

Discussion

Analysis of the available literature on MRI and MSCT revealed a considerable advantage for MSCT compared to MRI in the detection of CAD. A significant higher overall accuracy in the detection of coronary artery stenoses was demonstrated for MSCT as compared to MRI. In addition, an almost 17-fold elevated odds ratio was observed for an abnormal test result with MSCT, significantly higher than MRI ($P < 0.0001$). Linear-regression analysis revealed a better specificity for MSCT versus MRI in lower disease prevalence populations ($p = 0.056$). This is an important observation, since non-invasive imaging of the coronary arteries is most likely to be implemented as diagnostic tool to exclude CAD in patients with a low to intermediate likelihood of CAD, and thus to avoid the risks and expenses of invasive CAG in this particular patient group.

Although MRI has become an established modality in the non-invasive evaluation of many cardiac parameters, including ventricular function, myocardial perfusion and mass, our analysis suggests that concerning coronary imaging the technique is currently outperformed by MSCT. Despite initial promising results, diagnostic accuracy was significantly less compared to MSCT studies. However, it should be taken into account that both technologies are in a constant evolutionary state. For instance, the introduction of 3 Tesla systems may increase the resolution of MRI sufficiently to allow

improved detection of CAD⁵⁴. With MSCT on the other hand, the number of detector rows has increased from 4 to 64 and further expansion to 128 will soon be realized. This will result in faster acquisition times, enabling the coverage of the whole heart in less than 10 seconds. With these systems, breathing artefacts or breath-hold associated increases in heart rate during acquisition are less likely to occur. Indeed, studies performed with 16-slice technology show an increase in the number of evaluable segments as well as diagnostic accuracy as compared to results obtained with 4-slice systems (Table 3). Still, several important limitations exist, including the relatively high radiation exposure (which will increase slightly with more detector rows) and the limited value in patients with heart rates above 65³⁷ or with tachy-arrhythmias (for which reasons beta-blockers are frequently administered). The use of multi-segmented reconstruction algorithms, which are available on certain MSCT systems, may allow the inclusion of patients with higher heart rates without loss in temporal resolution or need for beta-blockade^{44;55}.

Another limitation of MSCT is that currently the technique does not allow quantification of stenosis severity. Eventually reliable absolute measurements of vessel diameter and lesion severity, similar to quantitative coronary angiography, will be needed. Nevertheless, a reliable estimate of overall coronary plaque burden can already be derived from MSCT. Indeed, the technique shows a clear potential for plaque characterization^{56;57}. Several studies comparing MSCT to intravascular ultrasound imaging, have shown a relation between the average Hounsfield Unit of the coronary plaque and its echogenicity, suggesting that MSCT can distinguish between soft, intermediate and calcified plaque^{56;57}.

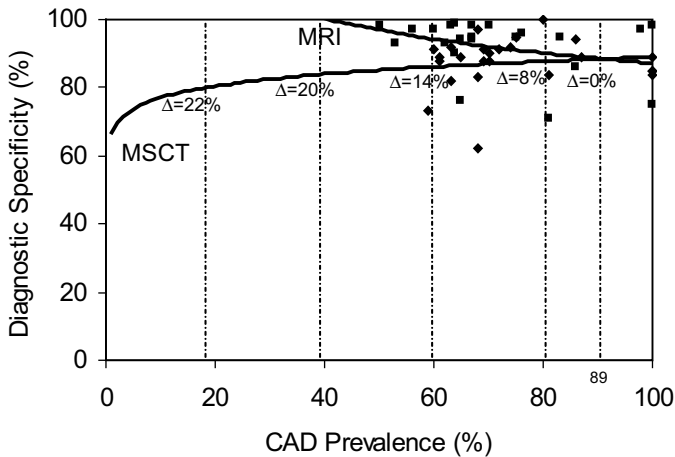


Figure 3. Relationship between CAD prevalence and diagnostic specificity for MSCT and MRI. Diagnostic specificity is plotted with a line of best fit within a range from >50% to 100% and predicted across a range of CAD prevalence rates from 10% to 50%.

Clinical implications

Because of its invasive nature and cost, indications for catheter-based diagnostic CAG have been restricted to a small fraction of high-risk patients with high pre-test likelihood of CAD. These patients are usually selected by risk-stratification and prior non-invasive imaging. Therefore, in current practice, coronary anatomy remains unknown in the majority of patients with CAD as well as in all asymptomatic subjects with a high-risk profile, frequently resulting in suboptimal therapy. The emergence of non-invasive diagnostic angiography by MSCT will grant the opportunity to obtain anatomic information about the coronary atherosclerotic process at a pre-clinical stage on a large scale. This is likely to have a profound impact on the practice of cardiology, in particular in the fields of revascularization on the one end, and prevention on the other end of the spectrum. Limited information is currently available on the accuracy of MSCT in low- and intermediate-prevalence populations, although extrapolation of the available data (Figure 3) suggests no loss in specificity of MSCT with decreasing disease prevalence. This observation suggests that the presence of CAD can be excluded with high accuracy such that the use of MSCT as a first-line evaluation tool could now be tested prospectively in selected subgroups.

Conclusion

Meta-analysis of available studies with MRI and MSCT for non-invasive coronary angiography indicates that MSCT has currently a significantly higher accuracy to detect or exclude significant CAD. MSCT may be considered the technique of choice to non-invasively evaluate coronary artery anatomy.

References

1. Krone RJ, Johnson L, Noto T. Five year trends in cardiac catheterization: a report from the Registry of the Society for Cardiac Angiography and Interventions. *Cathet Cardiovasc Diagn.* 1996;39:31-35.
2. Scanlon PJ, Faxon DP, Audet AM, Carabello B, Dehmer GJ, Eagle KA, Legako RD, Leon DF, Murray JA, Nissen SE, Pepine CJ, Watson RM, Ritchie JL, Gibbons RJ, Cheitlin MD, Gardner TJ, Garson A, Jr., Russell RO, Jr., Ryan TJ, Smith SC, Jr. ACC/AHA guidelines for coronary angiography. A report of the American College of Cardiology/American Heart Association Task Force on practice guidelines (Committee on Coronary Angiography). Developed in collaboration with the Society for Cardiac Angiography and Interventions. *J Am Coll Cardiol.* 1999;33:1756-1824.
3. Bogaert J, Kuzo R, Dymarkowski S, Beckers R, Piessens J, Rademakers FE. Coronary artery imaging with real-time navigator three-dimensional turbo-field-echo MR coronary angiography: initial experience. *Radiology.* 2003;226:707-716.
4. Sommer T, Hackenbroch M, Hofer U, Schmiedel A, Willinek WA, Flacke S, Gieseke J, Traber F, Fimmers R, Litt H, Schild H. Coronary MR Angiography at 3.0 T versus That at 1.5 T: Initial Results in Patients Suspected of Having Coronary Artery Disease. *Radiology.* 2005.
5. Muller MF, Fleisch M. Recurrent coronary artery stenosis: assessment with three-dimensional MR imaging. *J Magn Reson Imaging.* 2004;20:383-389.
6. Gerber BL, Coche E, Pasquet A, Ketelslegers E, Vancraeynest D, Grandin C, Van Beers BE, Vanoverschelde JL. Coronary artery stenosis: direct comparison of four-section multi-detector row CT and 3D navigator MR imaging for detection—initial results. *Radiology.* 2005;234:98-108.
7. Jahnke C, Paetsch I, Schnackenburg B, Bornstedt A, Gebker R, Fleck E, Nagel E. Coronary MR angiography with steady-state free precession: individually adapted breath-hold technique versus free-breathing technique. *Radiology.* 2004;232:669-676.
8. Ikonen AE, Manninen HI, Vainio P, Hirvonen TP, Vanninen RL, Matsi PJ, Soimakallio S, Hartikainen JE. Three-dimensional respiratory-gated coronary MR angiography with reference to X-ray coronary angiography. *Acta Radiol.* 2003;44:583-589.
9. Kessler W, Achenbach S, Moshage W, Zink D, Kroeker R, Nitz W, Laub G, Bachmann K. Usefulness of respiratory gated magnetic resonance coronary angiography in assessing narrowings > or = 50% in diameter in native coronary arteries and in aortocoronary bypass conduits. *Am J Cardiol.* 1997;80:989-993.
10. Kessler W, Laub G, Achenbach S, Ropers D, Moshage W, Daniel WG. Coronary arteries: MR angiography with fast contrast-enhanced three-dimensional breath-hold imaging—initial experience. *Radiology.* 1999;210:566-572.
11. Kim WY, Danias PG, Stuber M, Flamm SD, Plein S, Nagel E, Langerak SE, Weber OM, Pedersen EM, Schmidt M, Botnar RM, Manning WJ. Coronary magnetic resonance angiography for the detection of coronary stenoses. *N Engl J Med.* 2001;345:1863-1869.
12. Muller MF, Fleisch M, Kroeker R, Chatterjee T, Meier B, Vock P. Proximal coronary artery stenosis: three-dimensional MRI with fat saturation and navigator echo. *J Magn Reson Imaging.* 1997;7:644-651.
13. Plein S, Ridgway JP, Jones TR, Bloomer TN, Sivananthan MU. Coronary artery disease: assessment with a comprehensive MR imaging protocol—initial results. *Radiology.* 2002;225:300-307.
14. Post JC, van Rossum AC, Hofman MB, Valk J, Visser CA. Three-dimensional respiratory-gated MR angiography of coronary arteries: comparison with conventional coronary angiography. *AJR Am J Roentgenol.* 1996;166:1399-1404.
15. Regenfus M, Ropers D, Achenbach S, Schlundt C, Kessler W, Laub G, Moshage W, Daniel WG. Comparison of contrast-enhanced breath-hold and free-breathing respiratory-gated imaging in three-dimensional magnetic resonance coronary angiography. *Am J Cardiol.* 2002;90:725-730.
16. Sandstede JJ, Pabst T, Beer M, Geis N, Kenn W, Neubauer S, Hahn D. Three-dimensional MR coronary angiography using the navigator technique compared with conventional coronary angiography. *AJR Am J Roentgenol.* 1999;172:135-139.
17. Sardanelli F, Molinari G, Zandrino F, Balbi M. Three-dimensional, navigator-echo MR coronary angiography in detecting stenoses of the major epicardial vessels, with conventional coronary angiography as the standard of reference. *Radiology.* 2000;214:808-814.

18. van Geuns RJ, de Bruin HG, Rensing BJ, Wielopolski PA, Hulshoff MD, van Ooijen PM, Oudkerk M, de Feyter PJ. Magnetic resonance imaging of the coronary arteries: clinical results from three dimensional evaluation of a respiratory gated technique. *Heart*. 1999;82:515-519.
19. Watanabe Y, Nagayama M, Amoh Y, Fujii M, Fuku Y, Okumura A, Van Cauwenhove M, Stuber M, Dodo Y. High-resolution selective three-dimensional magnetic resonance coronary angiography with navigator-echo technique: segment-by-segment evaluation of coronary artery stenosis. *J Magn Reson Imaging*. 2002;16:238-245.
20. Weber C, Steiner P, Sinkus R, Dill T, Bornert P, Adam G. Correlation of 3D MR coronary angiography with selective coronary angiography: feasibility of the motion-adapted gating technique. *Eur Radiol*. 2002;12:718-726.
21. Wittlinger T, Voigtlander T, Rohr M, Meyer J, Thelen M, Kreitner KF, Kalden P. Magnetic resonance imaging of coronary artery occlusions in the navigator technique. *Int J Cardiovasc Imaging*. 2002;18:203-211.
22. Woodard PK, Li D, Haacke EM, Dhawale PJ, Kaushikkar S, Barzilai B, Braverman AC, Ludbrook PA, Weiss AN, Brown JJ, Mirowitz SA, Pilgram TK, Gutierrez FR. Detection of coronary stenoses on source and projection images using three-dimensional MR angiography with retrospective respiratory gating: preliminary experience. *AJR Am J Roentgenol*. 1998;170:883-888.
23. van Geuns RJ, Oudkerk M, Rensing BJ, Bongaerts AH, de Bruin HG, Wielopolski PA, van Ooijen P, de Feyter PJ, Serruys PW. Comparison of coronary imaging between magnetic resonance imaging and electron beam computed tomography. *Am J Cardiol*. 2002;90:58-63.
24. Manning WJ, Li W, Edelman RR. A preliminary report comparing magnetic resonance coronary angiography with conventional angiography. *N Engl J Med*. 1993;328:828-832.
25. Mohiaddin RH, Bogren HG, Lazim F, Keegan J, Gatehouse PD, Barbir M, Firmin DN, Yacoub MH. Magnetic resonance coronary angiography in heart transplant recipients. *Coron Artery Dis*. 1996;7:591-597.
26. Pennell DJ, Keegan J, Firmin DN, Gatehouse PD, Underwood SR, Longmore DB. Magnetic resonance imaging of coronary arteries: technique and preliminary results. *Br Heart J*. 1993;70:315-326.
27. Pennell DJ, Bogren HG, Keegan J, Firmin DN, Underwood SR. Assessment of coronary artery stenosis by magnetic resonance imaging. *Heart*. 1996;75:127-133.
28. Post JC, van Rossum AC, Hofman MB, de Cock CC, Valk J, Visser CA. Clinical utility of two-dimensional magnetic resonance angiography in detecting coronary artery disease. *Eur Heart J*. 1997;18:426-433.
29. Regenfus M, Ropers D, Achenbach S, Kessler W, Laub G, Daniel WG, Moshage W. Noninvasive detection of coronary artery stenosis using contrast-enhanced three-dimensional breath-hold magnetic resonance coronary angiography. *J Am Coll Cardiol*. 2000;36:44-50.
30. van Geuns RJ, Wielopolski PA, de Bruin HG, Rensing BJ, Hulshoff M, van Ooijen PM, de Feyter PJ, Oudkerk M. MR coronary angiography with breath-hold targeted volumes: preliminary clinical results. *Radiology*. 2000;217:270-277.
31. Achenbach S, Giesler T, Ropers D, Ulzheimer S, Derlien H, Schulte C, Wenkel E, Moshage W, Bautz W, Daniel WG, Kalender WA, Baum U. Detection of coronary artery stenoses by contrast-enhanced, retrospectively electrocardiographically-gated, multislice spiral computed tomography. *Circulation*. 2001;103:2535-2538.
32. Becker CR, Knez A, Leber A, Treede H, Ohnesorge B, Schoepf UJ, Reiser MF. Detection of coronary artery stenoses with multislice helical CT angiography. *J Comput Assist Tomogr*. 2002;26:750-755.
33. Knez A, Becker CR, Leber A, Ohnesorge B, Becker A, White C, Haberl R, Reiser MF, Steinbeck G. Usefulness of multislice spiral computed tomography angiography for determination of coronary artery stenoses. *Am J Cardiol*. 2001;88:1191-1194.
34. Kuettner A, Kopp AF, Schroeder S, Rieger T, Brunn J, Meisner C, Heuschmid M, Trabold T, Burgstahler C, Martensen J, Schoebel W, Selbmann HK, Claussen CD. Diagnostic accuracy of multidetector computed tomography coronary angiography in patients with angiographically proven coronary artery disease. *J Am Coll Cardiol*. 2004;43:831-839.
35. Leber AW, Knez A, Becker C, Becker A, White C, Thilo C, Reiser M, Haberl R, Steinbeck G. Non-Invasive intravenous coronary angiography using electron beam tomography and multislice computed tomography. *Heart*. 2003;89:633-639.
36. Morgan-Hughes GJ, Marshall AJ, Roobottom CA. Multislice Computed Tomographic Coronary Angiography: Experience in a UK Centre. *Clin Radiol*. 2003;58:378-383.
37. Nieman K, Rensing BJ, van Geuns RJ, Vos J, Pattynama PM, Krestin GP, Serruys PW, de Feyter PJ. Non-Invasive coronary angiography with multislice spiral computed tomography: impact of heart rate. *Heart*. 2002;88:470-474.

38. Nieman K, Rensing BJ, van Geuns RJ, Munne A, Ligthart JM, Pattynama PM, Krestin GP, Serruys PW, de Feyter PJ. Usefulness of multislice computed tomography for detecting obstructive coronary artery disease. *Am J Cardiol.* 2002;89:913-918.
39. Nieman K, Pattynama PM, Rensing BJ, van Geuns RJ, de Feyter PJ. Evaluation of patients after coronary artery bypass surgery: CT angiographic assessment of grafts and coronary arteries. *Radiology.* 2003;229:749-756.
40. Vogl TJ, Abolmaali ND, Diebold T, Engelmann K, Ay M, Dogan S, Wimmer-Greinecker G, Moritz A, Herzog C. Techniques for the detection of coronary atherosclerosis: multi-detector row CT coronary angiography. *Radiology.* 2002;223:212-220.
41. Maruyama T, Yoshizumi T, Tamura R, Takashima S, Toyoshima H, Konishi I, Yamashita S, Yamasaki K. Comparison of visibility and diagnostic capability of noninvasive coronary angiography by eight-slice multidetector-row computed tomography versus conventional coronary angiography. *Am J Cardiol.* 2004;93:537-542.
42. Matsuo S, Nakamura Y, Matsumoto T, Nakae I, Nagatani Y, Takazakura R, Takahashi M, Murata K, Horie M. Visual assessment of coronary artery stenosis with electrocardiographically-gated multislice computed tomography. *Int J Cardiovasc Imaging.* 2004;20:61-66.
43. Nieman K, Cademartiri F, Lemos PA, Raaijmakers R, Pattynama PM, de Feyter PJ. Reliable noninvasive coronary angiography with fast submillimeter multislice spiral computed tomography. *Circulation.* 2002;106:2051-2054.
44. Dewey M, Laule M, Krug L, Schnapauff D, Rogalla P, Rutsch W, Hamm B, Lembcke A. Multisegment and halfscan reconstruction of 16-slice computed tomography for detection of coronary artery stenoses. *Invest Radiol.* 2004;39:223-229.
45. Kuettner A, Trabold T, Schroeder S, Feyer A, Beck T, Brueckner A, Heuschmid M, Burgstahler C, Kopp AF, Claussen CD. Noninvasive detection of coronary lesions using 16-detector multislice spiral computed tomography technology: initial clinical results. *J Am Coll Cardiol.* 2004;44:1230-1237.
46. Kuettner A, Beck T, Drosch T, Kettering K, Heuschmid M, Burgstahler C, Claussen CD, Kopp AF, Schroeder S. Diagnostic accuracy of noninvasive coronary imaging using 16-detector slice spiral computed tomography with 188 ms temporal resolution. *J Am Coll Cardiol.* 2005;45:123-127.
47. Mollet NR, Cademartiri F, Nieman K, Saia F, Lemos PA, McFadden EP, Pattynama PM, Serruys PW, Krestin GP, de Feyter PJ. Multislice spiral computed tomography coronary angiography in patients with stable angina pectoris. *J Am Coll Cardiol.* 2004;43:2265-2270.
48. Schuijf JD, Bax JJ, Salm LP, Jukema JW, Lamb HJ, van der Wall EE, de Roos A. Noninvasive coronary imaging and assessment of left ventricular function using 16-slice computed tomography. *Am J Cardiol.* 2005;95:571-574.
49. Martuscelli E, Romagnoli A, D'Eliseo A, Razzini C, Tomassini M, Sperandio M, Simonetti G, Romeo F. Accuracy of thin-slice computed tomography in the detection of coronary stenoses. *Eur Heart J.* 2004;25:1043-1048.
50. Hoffmann U, Moselewski F, Cury RC, Ferencik M, Jang IK, Diaz LJ, Abbara S, Brady TJ, Achenbach S. Predictive value of 16-slice multidetector spiral computed tomography to detect significant obstructive coronary artery disease in patients at high risk for coronary artery disease: patient-versus segment-based analysis. *Circulation.* 2004;110:2638-2643.
51. Morgan-Hughes GJ, Roobottom CA, Owens PE, Marshall AJ. Highly accurate coronary angiography with submillimetre, 16 slice computed tomography. *Heart.* 2005;91:308-313.
52. Mollet NR, Cademartiri F, Krestin GP, McFadden EP, Arampatzis CA, Serruys PW, de Feyter PJ. Improved diagnostic accuracy with 16-row multi-slice computed tomography coronary angiography. *J Am Coll Cardiol.* 2005;45:128-132.
53. Ropers D, Baum U, Pohle K, Anders K, Ulzheimer S, Ohnesorge B, Schlundt C, Bautz W, Daniel WG, Achenbach S. Detection of coronary artery stenoses with thin-slice multi-detector row spiral computed tomography and multiplanar reconstruction. *Circulation.* 2003;107:664-666.
54. Nayak KS, Cunningham CH, Santos JM, Pauly JM. Real-time cardiac MRI at 3 tesla. *Magn Reson Med.* 2004;51:655-660.
55. Kachelriess M, Ulzheimer S, Kalender WA. ECG-correlated image reconstruction from subsecond multi-slice spiral CT scans of the heart. *Med Phys.* 2000;27:1881-1902.

56. Achenbach S, Moselewski F, Ropers D, Ferencik M, Hoffmann U, MacNeill B, Pohle K, Baum U, Anders K, Jang IK, Daniel WG, Brady TJ. Detection of calcified and noncalcified coronary atherosclerotic plaque by contrast-enhanced, submillimeter multidetector spiral computed tomography: a segment-based comparison with intravascular ultrasound. *Circulation*. 2004;109:14-17.
57. Schroeder S, Kopp AF, Baumbach A, Meisner C, Kuettner A, Georg C, Ohnesorge B, Herdeg C, Claussen CD, Karsch KR. Noninvasive detection and evaluation of atherosclerotic coronary plaques with multislice computed tomography. *J Am Coll Cardiol*. 2001;37:1430-1435.



Part II

Defining Patient Populations

II A

Coronary Risk Factors

Chapter 6

Non-Invasive Angiography and Assessment of Left Ventricular Function using Multi-slice Computed Tomography in Patients with Type 2 Diabetes

Joanne D. Schuijf, Jeroen J. Bax, J. Wouter Jukema, Hildo J. Lamb,
Hubert W. Vliegen, Liesbeth P. Salm, Albert de Roos,
Ernst E. van der Wall

Abstract

Background

Early identification of coronary artery disease (CAD) in patients with diabetes is important, since these patients are at elevated risk for developing CAD and have worse outcome as compared to non-diabetic patients, once diagnosed with CAD. Recently, non-invasive coronary angiography and assessment of left ventricular (LV) function has been demonstrated with multi-slice computed tomography (MSCT). The purpose of the present study was to validate this approach in patients with type 2 diabetes.

Methods

MSCT was performed in 30 patients with confirmed type 2 diabetes. From the MSCT images, coronary artery stenoses ($\geq 50\%$ luminal narrowing) and LV function (LV ejection fraction, regional wall motion) were evaluated and compared with conventional angiography and 2D-echocardiography.

Results

A total of 220 (86%) of 256 coronary artery segments were interpretable with MSCT. In these segments, sensitivity and specificity for the detection of coronary artery stenoses were 95%. Including the uninterpretable segments, sensitivity and specificity were 81% and 82%, respectively. Bland-Altman analysis in the comparison of LV ejection fractions demonstrated a mean difference of $-0.48\% \pm 3.8\%$ for MSCT and echocardiography, not significantly different from zero. Agreement between the 2 modalities for assessment of regional contractile function was excellent (91%, kappa statistic 0.81).

Conclusion

Accurate non-invasive evaluation of both the coronary arteries and LV function with MSCT is feasible in patients with type 2 diabetes. This non-invasive approach may allow optimal identification of high-risk patients.

Introduction

Type 2 diabetes is a major risk factor for coronary artery disease (CAD) and is associated with a 2- to 4- fold increase in the risk of developing CAD ¹. Furthermore, prognosis of patients with type 2 diabetes and confirmed CAD has been demonstrated to be worse than in non-diabetic patients with CAD. For example, the likelihood of developing myocardial infarction is significantly higher in diabetic patients with unstable angina compared to non-diabetic individuals. Moreover, mortality rate after myocardial infarction has also been shown to be doubled ². Early identification of CAD is therefore of paramount importance in patients with diabetes.

Non-invasive testing including myocardial perfusion scintigraphy and dobutamine stress echocardiography have been used to detect CAD ^{3,4}. However, direct visualization of the coronary arteries may be preferred since patients with diabetes frequently have diffuse, multi-vessel CAD. Currently, conventional angiography is performed to evaluate the presence and extent of CAD. However, this is an invasive approach associated with a minimal but definitive risk of complications, and a non-invasive technique that is capable of direct visualization of the coronary arteries would be preferred. A promising new imaging technique for the non-invasive detection of CAD is multi-slice computed tomography (MSCT), which allows the acquisition of high quality images of the entire heart within a single breath-hold. Several studies have demonstrated the technique to be useful in the detection of coronary artery stenoses with sensitivities and specificities ranging from 72% to 95% and 75% to 99%, respectively ⁵⁻¹¹.

In addition, MSCT allows simultaneous assessment of left ventricular (LV) function, which also is an important prognostic parameter ⁴. Although the studies on assessment of LV function with MSCT are scarce, the initial results demonstrated a good relation between LV ejection fraction assessed by MSCT and 2D-echocardiography or Magnetic Resonance Imaging (MRI) ¹²⁻¹⁴.

Combined assessment of LV function and the coronary artery status with MSCT may allow optimal non-invasive evaluation of patients with diabetes with suspected CAD. Thus far, the value of MSCT has not been evaluated in patients with diabetes. Accordingly, the purpose of the present study was to perform a combined assessment of coronary arteries and LV function in patients with type 2 diabetes using MSCT; the results were compared to conventional angiography and 2D-echocardiography, respectively.

Methods

Patients and study protocol

The study group consisted of 30 patients with known type 2 diabetes who were scheduled for conventional angiography because of anginal complaints. Criteria for the diagnosis of diabetes were, as recommended by the American Diabetes Association¹⁵:

1. symptoms of diabetes plus casual plasma glucose concentration ≥ 200 mg/dl (11.1 mmol/l) or
2. fasting plasma glucose level ≥ 126 mg/dl (7.0 mmol/l).

Exclusion criteria were: atrial fibrillation, renal insufficiency (serum creatinine >120 mmol/L), known allergy to iodine contrast media, severe claustrophobia and pregnancy.

The average interval between conventional angiography and MSCT was 17 ± 27 days, whereas 2D-echocardiography was performed prior or after the CT examination within two weeks. All patients gave written informed consent to the study protocol, which was approved by the local ethics committee.

MSCT; Data acquisition

In the initial 12 patients, MSCT was performed using a Toshiba Multi-Slice Aquilion 0.5 (collimation 4×2.0 mm) system and in the remaining 18 patients using a Toshiba Multi-slice Aquilion 16 system (collimation 16×0.5 mm) (Toshiba Medical Systems, Otawara, Japan). Rotation time was 0.4s or 0.5s, depending on the heart rate, while the tube current was 250 mA, at 120 kV. A bolus of 140 ml contrast (Xenetix 300°, Guerbet, Aulnay S. Bois, France) was administered with an injection rate of 4 ml/s in the antecubital vein. To time the scan, automated peak enhancement detection in the aortic root was used. The heart was imaged from the aortic root to the cardiac apex during inspiratory breath hold, while the ECG was recorded simultaneously for retrospective gating of the data. To assess LV function, 20 cardiac phases were reconstructed in the short-axis orientation with a slice thickness of 2.00 mm and subsequently transferred to a remote workstation with dedicated cardiac software (MR Analytical Software System [MASS], Medis, Leiden, the Netherlands).

To evaluate the coronary arteries, 5 reconstructions covering diastole (65% - 85% of the R-R range) were generated with a slice thickness of either 1.0 mm (4-slice system) or 0.5 mm (16-slice system). If motion artifacts were present, additional reconstructions were made at 40%, 45% and 50% of the cardiac cycle. Images were transferred to a remote workstation (Vitrea2, Vital Images, Plymouth, Minn. USA) for post-processing.

MSCT; Data analysis

Stenosis assessment was performed using a modified AHA-ACC segmentation model: the left main coronary artery (segment 5), the right coronary artery (segments 1, 2, 3, and if present 4 and 16), the left anterior descending coronary artery (segments 6,7, 8, and 9), and the left circumflex artery

(segment 11, 13, and if present 12, 14, 15, and 17). Only side-branches of ≥ 1.5 mm as determined by quantitative coronary angiography or supplied by coronary bypass grafts were evaluated. Images were evaluated by an experienced observer blinded to the catheterization results, using both the original axial MSCT images and curved multiplanar reconstructions. Each segment was first evaluated as interpretable or not. Subsequently, the presence of significant narrowing ($\geq 50\%$ reduction of lumen diameter) was determined in the assessable segments. In addition, coronary bypass grafts, if present, were evaluated for the presence of $\geq 50\%$ luminal narrowing or not. In those patients, native coronary segments prior to the anastomosis of a patent graft, were not evaluated.

Regional wall motion was assessed visually using the short-axis slices (displayed in cine-loop format) by one observer blinded to all other data using a previously described 17-segment model¹⁶. Each segment was assigned a wall motion score using a 4-point scale (1=normokinesia, 2=hypokinesia, 3=akinesia, and 4=dyskinesia). LV ejection fraction was calculated using semi-automated endocardial contour detection, with manual correction when necessary. Papillary muscles were regarded as being part of the LV cavity.

Conventional angiography

Conventional angiography was performed according to standard techniques. Vascular access was obtained by using the femoral approach with the Seldinger technique.

Coronary angiograms were visually evaluated by an experienced observer blinded to the MSCT data.

2D-echocardiography

Patients were imaged in the left lateral decubitus position using a commercially available system (Vingmed System FiVe/Vivid-7, GE-Vingmed, Milwaukee, WI, USA). Images were acquired using a 3.5 MHz transducer at a depth of 16 cm in the parasternal and apical views.

Regional wall motion was analyzed using the same 17-segment model and 4-point scale as described above. LV ejection fractions were calculated from the 2- and 4-chamber images using the biplane Simpson's rule¹⁷.

Statistical analysis

Sensitivity, specificity, positive and negative predictive values for the detection of significant coronary artery stenoses were calculated. In addition, a patient based analysis was performed. MSCT was considered correct in the individual patient analysis if at least one significant stenosis was detected on the MSCT images or if MSCT ruled out the presence of any significant stenosis. Pre-test likelihood of CAD in patients without previous myocardial infarction or coronary bypass grafting was estimated using the Diamond-Forrester method¹⁸. Bland-Altman analysis was performed for each pair of values of LV ejection fraction to calculate limits of agreement and systematic error between the

two modalities¹⁹. Agreement for regional wall motion was expressed in a 4x4 table using weighted kappa statistics. A kappa value of <0.4 represents poor agreement, a kappa value between 0.4 and 0.75 fair to good agreement, and a kappa value of >0.75 is considered an excellent agreement, based on the Fleiss' classification²⁰. A p-value <0.05 was considered to indicate statistical significance.

Results

Patient characteristics

The patient characteristics are summarized in Table 1. The study group consisted of 30 patients (26 men, mean age 62 ± 10 years) with type 2 diabetes. The average duration of diabetes mellitus was 2.9 ± 4.4 years at the time of MSCT. A total of 11 patients received oral hypoglycaemic medication or insulin (n=5). Cardiac medication was continued during the study period. A total of 16 (53%) patients used beta-blocking agents, and no additional beta-blocking agents were administered in preparation of the scan.

Table 1. Clinical characteristics of the study population (n=30).

	n (%)
Gender (M/F)	26/4
Age (years)	62 ± 10
Beta-blocking medication	16 (53)
Heart rate during acquisition	69 ± 13
Diabetes type 2	30 (100)
Average HbA _{1c}	$6.9\% \pm 1.4\%$
Other risk factors for CAD	
Hypertension	16 (73)
Smoking	12 (56)
Hypercholesterolemia	21 (95)
Family with CAD	12 (56)
History	
Previous MI	20 (67)
Previous PCI/CABG	21 (70)/11 (37)
Vessel disease	
1-vessel	6 (20)
2-vessel	6 (20)
3-vessel	16 (53)
Angina Pectoris	
CCS class 1/2	7 (23)
CCS class 3/4	23 (77)
Heart Failure	
NYHA class 1/2	25 (83)
NYHA class 3/4	5 (17)

CABG: coronary artery bypass grafting; CCS: Canadian Cardiovascular Society; MI: myocardial infarction; NYHA: New York Heart Association; PCI: percutaneous coronary intervention.

Coronary artery stenoses

A total of 256 coronary segments were present for evaluation by both MSCT and conventional angiography. Of the 99 segments studied with 4-slice MSCT, 18 (18%) were uninterpretable, whereas also 18 (11%) of 157 segments acquired with 16-slice MSCT were of non-diagnostic quality. Thus, 36 (14%) segments were classified uninterpretable. In the remaining 220 segments, conventional angiography revealed 59 significant ($\geq 50\%$ diameter reduction) lesions. Evaluation of the MSCT images resulted in the correct identification of 56 (95%) stenoses. In 153 of 161 (95%) segments, the presence of significant stenosis was correctly ruled out. Thus, resulting sensitivity and specificity were 95%. When the uninterpretable segments were included in the analysis, resulting sensitivity and specificity were 81% and 82%, respectively.

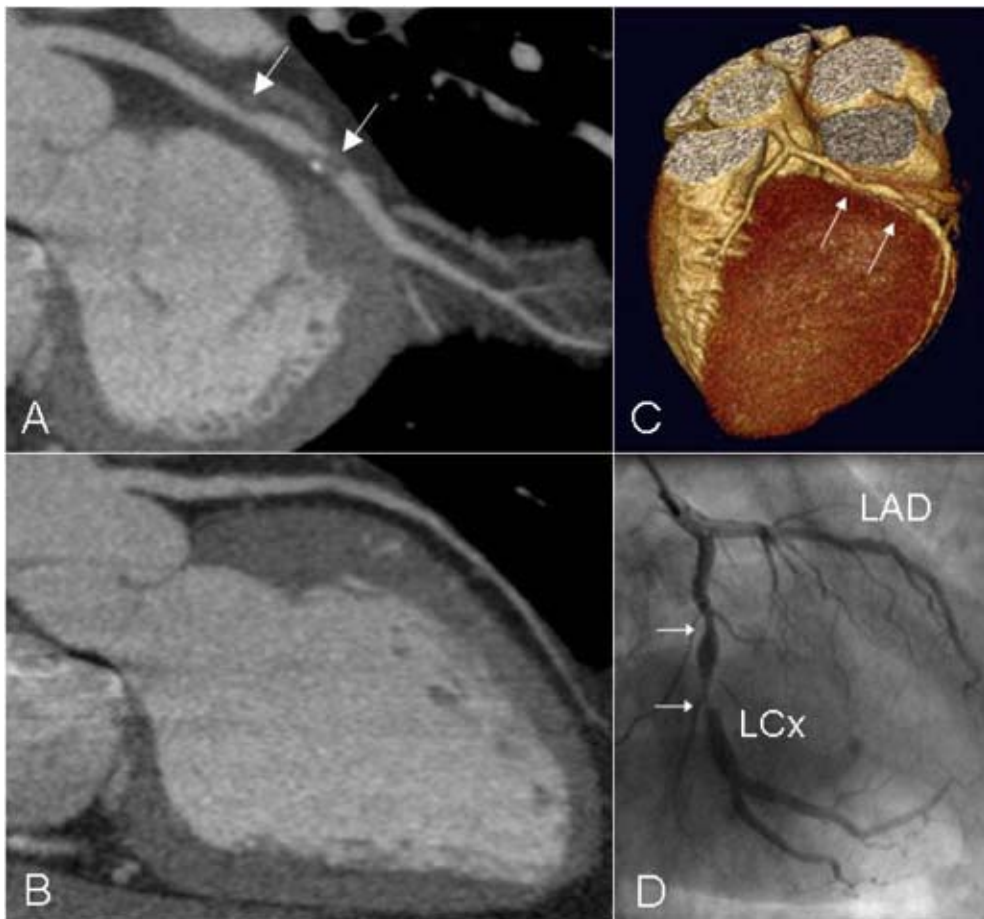


Figure 1. In panel A, a curved multiplanar reconstruction of a left circumflex coronary artery (LCx) with severe narrowing of the lumen is depicted. No abnormalities however were observed in the left anterior descending coronary artery (LAD) of this patient (panel B). Also, in the 3D volume rendered reconstruction (panel C), stenoses in the LCx as well as patency of the LAD are clearly visible. Findings were confirmed by conventional X-ray angiography (panel D).

A total of 21 grafts were present (arterial=5, venous=16). Conventional angiography revealed the presence of $\geq 50\%$ luminal narrowing in 9 grafts. MSCT correctly identified all 9 grafts with significant stenosis, whereas 9 of 12 grafts without significant stenosis were correctly identified on the MSCT images. In the 3 remaining grafts however the presence of significant narrowing could not be evaluated, although patency of the graft could be assessed correctly.

On a per patient basis, MSCT was accurate in 26 (87%) of 30 patients. In 7 patients, no significant abnormalities were observed during conventional angiography, and 5 (71%) of these patients were correctly identified as having no significant lesions using the MSCT images. Of the remaining 23 patients with significant lesions on conventional angiography, 21 (91%) were correctly identified using MSCT. In 23 patients CAD was known. In the remaining 7 patients with suspected CAD, the pre-test likelihood according to Diamond-Forrester was intermediate in 2 and high in 5 patients. Conventional angiography demonstrated the presence of significant lesions in 5 patients, of which 4 (80%) were correctly identified with MSCT. Of the 2 patients without significant CAD, 1 (50%) was correctly assessed with MSCT.

Examples of MSCT images of both a stenotic and non-stenotic coronary artery with the corresponding angiographic images are shown in Figure 1.

LV function

From one patient, MSCT data were lost (due to technical errors) after successful acquisition, and therefore data from 29 patients were available for LV function analysis.

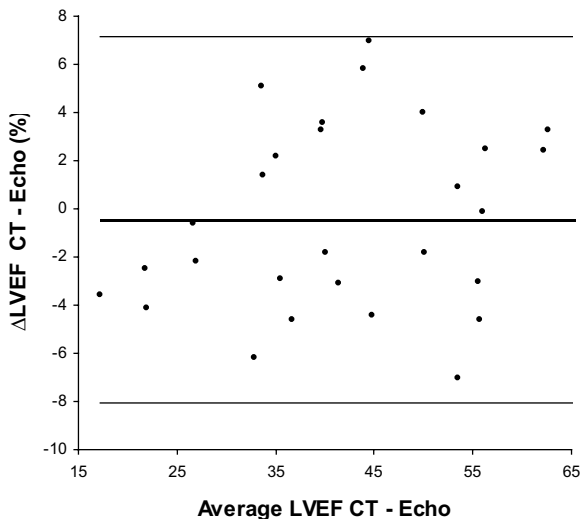


Figure 2. Bland-Altman plot in the comparison of MSCT and echocardiography in the assessment of LV ejection fraction.

The difference between each pair is plotted against the average value of the same pair (solid line= mean value of differences and dotted lines = mean value of differences ± 2 SDs).

Global function

Mean LV ejection fraction, as determined by echocardiography and MSCT, was $43\% \pm 14\%$ (range: 19% - 75%) and $43\% \pm 14\%$ (range: 15% - 72%, ns), respectively. Bland-Altman analysis in the comparison of CT and echo LV ejection fraction demonstrated a mean difference of $-0.48\% \pm 3.8\%$, not significantly different from zero (Figure 2).

Regional function

Echocardiography revealed contractile dysfunction in 157 (32%) of 493 segments, with 71 (45%) showing hypokinesia, 74 (47%) akinesia and 12 (8%) dyskinesia. In 149 (95%) of the dysfunctional segments, decreased systolic wall thickening was also observed on the MSCT images. An excellent agreement was shown between the two techniques, with 91% of segments scored identically on both modalities (kappa statistic 0.81 ± 0.03). Agreements for the individual gradings (1-4) were 97%, 82%, 73%, and 92%, respectively. In Figure 3, examples of short-axis reconstructions are shown, illustrating patients with and without wall motion abnormalities.

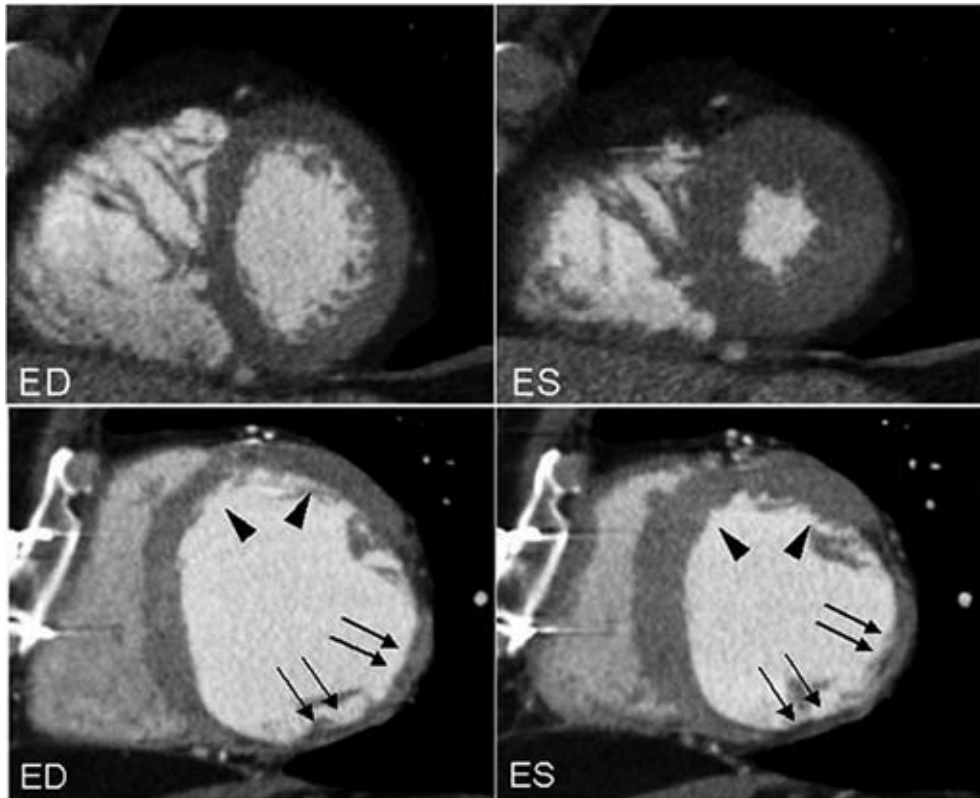


Figure 3. MSCT short-axis reconstructions in end-diastole (ED, left panels) and end-systole (ES, right panels). In the upper two panels (A), normal systolic wall thickening is clearly present in all segments. In the lower two panels, short-axis reconstructions of a patient with a previous inferolateral infarction are shown. Although preserved wall motion is still present in the anterior region (arrowheads), akinesia of the severely thinned wall is clearly visible in the infarcted region (arrows) (B).

Discussion

Our study demonstrates that non-invasive coronary angiography is feasible in patients with diabetes. An excellent sensitivity and specificity of both 95% were shown for the detection of coronary artery stenoses. Corresponding positive and negative predictive values were 88% and 98%, respectively. With inclusion of the uninterpretable segments, sensitivity and specificity were still 81% and 82%, respectively. Moreover, although inclusion of uninterpretable segments resulted in a positive predictive value of 62%, the negative predictive value remained high (92%), which is in line with previous studies^{11,21}. This is an important finding, since clinical management is often difficult in patients presenting with diabetes and suspected CAD. In a substantial number of patients, non-invasive tests are inconclusive and knowledge of coronary anatomy (by means of invasive angiography) is often needed in order to determine the most optimal treatment strategy. The high accuracy of MSCT in the exclusion of CAD as demonstrated by the high specificity and negative predictive value in the current study underscores the potential of this technique to function as a first-line diagnostic modality in the workup of patients with suspected CAD. By ruling out the presence of significant stenoses, risks and costs of invasive angiography can thus be avoided in a substantial number of patients. Moreover, accurate information of coronary anatomy and extent of atherosclerosis as well as cardiac function is obtained, which may optimize treatment strategy and prognostication and may eventually even serve as a guide for interventional procedures. However, further prognostic studies are needed in larger cohorts before MSCT can become an established diagnostic tool and replace conventional coronary angiography in certain patient groups.

In addition, LV function analysis was performed after retrospective reconstruction of the acquired data. In the assessment of LV ejection fraction, a close correlation was observed between MSCT and 2D-echocardiography. Mean LV ejection fraction as determined by MSCT was slightly less as compared to the echocardiographic results, but no statistical difference was reached. A slight underestimation of LV ejection fraction with MSCT has been reported previously¹²⁻¹⁴ which may be attributed to an overestimation of LV end-systolic volume. Since minimal ventricular volume is maintained for only 80-200 ms, temporal resolution of MSCT may not have been sufficient in all patients.

Overall agreement of regional wall motion score was excellent with 91% of segments scored identically. The agreement for the individual wall motion scores was highest in the extremes, i.e. in segments with either normal contractility (97%) or dyskinesia (92%), whereas it was slightly lower in segments showing intermediate contractile dysfunction. Since MSCT is most likely to be applied as a first line screening tool, baseline LV function may be used to further refine risk stratification in the individual patient. However, it does currently not offer an alternative to echocardiographic examination since evaluation of valvular or diastolic function is not possible with MSCT.

Some limitations of the current study need to be acknowledged. First, in the present study only 30 patients were included. Studies in larger patients cohorts are needed to precisely determine the accuracy of MSCT in patients with type 2 diabetes.

Second, LV function analysis was compared to 2D-echocardiography instead of MRI, which is considered the current gold standard for evaluation of LV function. In contrast to MRI, 2D-echocardiogra-

phy relies on geometrical assumptions and may thus be somewhat less accurate. Still, our results are very similar to those obtained in the few available comparisons between MSCT and MRI^{13;14}. Third, in the present study 14% of coronary segments were uninterpretable, which is in line with previous studies^{6;11;22}. However, with the introduction of 32- and 64-slice systems the percentage of uninterpretable segments is likely to decline further.

Fourth, although some authors have recommended the use of beta-blocking agents⁷, no additional beta-blocking agents were administered prior to the examination in the present study. The use of a multi-segmented reconstruction algorithm, which is available on our MSCT equipment, allowed the inclusion of patients with heart rates higher than 65 beats per minutes without loss in temporal resolution²³. Furthermore, additional administration of beta-blocking agents may have interfered with cardiac function analysis, rendering it less reliable.

Finally, a major drawback of MSCT remains the radiation dose, which is approximately 6-9 mSv²⁴⁻²⁶. The development of new filters and optimized acquisition protocols will lead to a substantial reduction of radiation dose.

In conclusion, accurate non-invasive evaluation of both the coronary arteries and LV function with MSCT is feasible in patients with type 2 diabetes. This combined strategy may improve the non-invasive evaluation of CAD in this particular patient group.

References

1. Luscher TF, Creager MA, Beckman JA, Cosentino F. Diabetes and vascular disease: pathophysiology, clinical consequences, and medical therapy: Part II. *Circulation*. 2003;108:1655-1661.
2. Herlitz J, Karlson BW, Lindqvist J, Sjolín M. Rate and mode of death during five years of follow-up among patients with acute chest pain with and without a history of diabetes mellitus. *Diabet Med*. 1998;15:308-314.
3. Schinkel AF, Elhendy A, Van Domburg RT, Bax JJ, Vourvouri EC, Sozzi FB, Valkema R, Roelandt JR, Poldermans D. Prognostic value of dobutamine-atropine stress myocardial perfusion imaging in patients with diabetes. *Diabetes Care*. 2002;25:1637-1643.
4. Sozzi FB, Elhendy A, Roelandt JR, Van Domburg RT, Schinkel AF, Vourvouri EC, Bax JJ, De Sutter J, Borghetti A, Poldermans D. Prognostic value of dobutamine stress echocardiography in patients with diabetes. *Diabetes Care*. 2003;26:1074-1078.
5. Achenbach S, Giesler T, Ropers D, Ulzheimer S, Derlien H, Schulte C, Wenkel E, Moshage W, Bautz W, Daniel WG, Kalender WA, Baum U. Detection of coronary artery stenoses by contrast-enhanced, retrospectively electrocardiographically-gated, multislice spiral computed tomography. *Circulation*. 2001;103:2535-2538.
6. Leber AW, Knez A, Becker C, Becker A, White C, Thilo C, Reiser M, Haberl R, Steinbeck G. Non-invasive intravenous coronary angiography using electron beam tomography and multislice computed tomography. *Heart*. 2003;89:633-639.
7. Nieman K, Rensing BJ, van Geuns RJ, Vos J, Pattynama PM, Krestin GP, Serruys PW, de Feyter PJ. Non-invasive coronary angiography with multislice spiral computed tomography: impact of heart rate. *Heart*. 2002;88:470-474.
8. Nieman K, Cademartiri F, Lemos PA, Raaijmakers R, Pattynama PM, de Feyter PJ. Reliable noninvasive coronary angiography with fast submillimeter multislice spiral computed tomography. *Circulation*. 2002;106:2051-2054.
9. Nieman K, Rensing BJ, van Geuns RJ, Munne A, Ligthart JM, Pattynama PM, Krestin GP, Serruys PW, de Feyter PJ. Usefulness of multislice computed tomography for detecting obstructive coronary artery disease. *Am J Cardiol*. 2002;89:913-918.
10. Nieman K, Pattynama PM, Rensing BJ, van Geuns RJ, de Feyter PJ. Evaluation of patients after coronary artery bypass surgery: CT angiographic assessment of grafts and coronary arteries. *Radiology*. 2003;229:749-756.
11. Ropers D, Baum U, Pohle K, Anders K, Ulzheimer S, Ohnesorge B, Schlundt C, Bautz W, Daniel WG, Achenbach S. Detection of coronary artery stenoses with thin-slice multi-detector row spiral computed tomography and multiplanar reconstruction. *Circulation*. 2003;107:664-666.
12. Dirksen MS, Bax JJ, de Roos A, Jukema JW, van der Geest RJ, Geleijns K, Boersma E, van der Wall EE, Lamb HJ. Usefulness of dynamic multislice computed tomography of left ventricular function in unstable angina pectoris and comparison with echocardiography. *Am J Cardiol*. 2002;90:1157-1160.
13. Mahnken AH, Spuentrup E, Niethammer M, Buecker A, Boese J, Wildberger JE, Flohr T, Sinha AM, Krombach GA, Gunther RW. Quantitative and qualitative assessment of left ventricular volume with ECG-gated multislice spiral CT: value of different image reconstruction algorithms in comparison to MRI. *Acta Radiol*. 2003;44:604-611.
14. Juergens KU, Grude M, Maintz D, Fallenberg EM, Wichter T, Heindel W, Fischbach R. Multi-detector row CT of left ventricular function with dedicated analysis software versus MR imaging: initial experience. *Radiology*. 2004;230:403-410.
15. Diagnosis and classification of diabetes mellitus. *Diabetes Care*. 2004;27 Suppl 1:S5-S10.
16. Cerqueira MD, Weissman NJ, Dilsizian V, Jacobs AK, Kaul S, Laskey WK, Pennell DJ, Rumberger JA, Ryan T, Verani MS. Standardized myocardial segmentation and nomenclature for tomographic imaging of the heart: a statement for healthcare professionals from the Cardiac Imaging Committee of the Council on Clinical Cardiology of the American Heart Association. *Circulation*. 2002;105:539-542.
17. Schiller NB, Acquatella H, Ports TA, Drew D, Goerke J, Ringertz H, Silverman NH, Brundage B, Botvinick EH, Boswell R, Carlsson E, Parmley WW. Left ventricular volume from paired biplane two-dimensional echocardiography. *Circulation*. 1979;60:547-555.
18. Diamond GA, Forrester JS. Analysis of probability as an aid in the clinical diagnosis of coronary-artery disease. *N Engl J Med*. 1979;300:1350-1358.

19. Bland JM, Altman DG. Statistical methods for assessing agreement between two methods of clinical measurement. *Lancet*. 1986;1:307-310.
20. Fleiss JL. Statistical methods for Rates and proportions. Second edition. New York: Wiley 1981.
21. Martuscelli E, Romagnoli A, D'Eliseo A, Razzini C, Tomassini M, Sperandio M, Simonetti G, Romeo F. Accuracy of thin-slice computed tomography in the detection of coronary stenoses. *Eur Heart J*. 2004;25:1043-1048.
22. Maruyama T, Yoshizumi T, Tamura R, Takashima S, Toyoshima H, Konishi I, Yamashita S, Yamasaki K. Comparison of visibility and diagnostic capability of noninvasive coronary angiography by eight-slice multidetector-row computed tomography versus conventional coronary angiography. *Am J Cardiol*. 2004;93:537-542.
23. Dewey M, Laule M, Krug L, Schnapauff D, Rogalla P, Rutsch W, Hamm B, Lembcke A. Multisegment and halfscan reconstruction of 16-slice computed tomography for detection of coronary artery stenoses. *Invest Radiol*. 2004;39:223-229.
24. Hunold P, Vogt FM, Schmermund A, Debatin JF, Kerkhoff G, Budde T, Erbel R, Ewen K, Barkhausen J. Radiation exposure during cardiac CT: effective doses at multi-detector row CT and electron-beam CT. *Radiology*. 2003;226:145-152.
25. Trabold T, Buchgeister M, Kuttner A, Heuschmid M, Kopp AF, Schroder S, Claussen CD. Estimation of radiation exposure in 16-detector row computed tomography of the heart with retrospective ECG-gating. *Rofo Fortschr Geb Rontgenstr Neuen Bildgeb Verfahr*. 2003;175:1051-1055.
26. Bae KT, Hong C, Whiting BR. Radiation dose in multidetector row computed tomography cardiac imaging. *J Magn Reson Imaging*. 2004;19:859-863.

